Journal of Materials Chemistry C

PAPER

View Article Online
View Journal | View Issue

Cite this: J. Mater. Chem. C, 2017, 5, 5083

White emission thin films based on rationally designed supramolecular coordination polymers†

Jinghui Yang,[a] Yun Yan,[b] Yonghai Hui*[a] and Jianbin Huang*[ab]

Received 4th April 2017,
Accepted 28th April 2017

DOI: 10.1039/c7tc01429e

rsc.li/materials-c

Fabrication of solid white luminescent materials is a challenging topic. In this work we report that upon combining the advantages of aggregation induced emission and reversible coordination polymers, solid white luminescent films with the CIE coordinates of (0.335, 0.347) and external quantum efficiencies of up to 11.74% can be achieved *via* layer-by-layer assembly. In particular, the ratio of the R(red) G(green) B(blue) elements can be rationally controlled *via* concentration, demonstrating the advantage of reversible coordination polymers in the fabrication of functional materials. The white emission of the solid thin film displays excellent stability against temperature, pH, and explosion materials, but exhibits specific detection for Cl_2, suggesting its great potential for application as both a robust luminescent material and a chemical sensor.

Introduction

White emission materials have attracted considerable interest in the last decade owing to their potential application as luminescent materials[1,2] and chemical sensors.[3–5] Because white light can be regarded as a balanced composition of red (R), green (G), and blue (B) colors at specific intensity ratios, any change in one color intensity can produce detectable, off-white emission.[6] For this reason, sensors based on white emitting materials are expected to be extremely sensitive to analyses.

The central issue for constructing white emission materials is the specific intensity ratio between RGB colors. In principle, materials suitable for the construction of light emissions can be achieved with infinite compositions.[7–9] For instance, metal–organic frameworks,[10,11] quantum dots,[12,13] lanthanide doped systems,[14,15] and mixtures of organic dyes[16–18] are all reported for the successful generation of white emission systems. However, most of the aforementioned systems are formed in liquid, and function in the form of suspensions or hydrogels. From the application point of view, solid-state emission materials could enable long-term stability during storage and transport,[19] among which, film materials are especially desired since they possess a large surface area and consume minimum working materials.

As a convenient technique of film generation, layer-by-layer (LBL) assembly employs oppositely charged polycharged molecules, usually various polyelectrolytes, to alternatively assemble on a solid surface. This allows preparing highly homogeneous films from water solution, which is of crucial significance for economic and environmental considerations. Furthermore, the layer-by-layer assembly can generate films with tailored thickness,[20] composites, and functionality.[21–23] So far, LBL assembly has been successfully employed in the construction of various fluorescent microcapsules[24–26] and films.[27–29] However, white light emitting films still remain challenging, since few fluorescent materials, except quantum dots,[30,31] are accessible for LBL assembly. Therefore, it is highly desired to explore other materials for the fabrication of LBL white emission films.

Recently, reversible coordination polymers have emerged as an attractive family of supramolecular polyelectrolytes which can be used for ionic self-assembly.[32–38] Different from those covalent polymers or polymeric structures based on an inert coordination bond, the connection between the ligand and the metal ions are reversible and dynamic, which allows facile incorporation of versatile metal ions and organic functional groups into polymeric structures.[32,39–41] We have shown that this unique structural and compositional character make them very capable in building up advanced structures with desired functions,[42–48] especially the controlled mixing of metal ions in the electrostatic assembly of coordination polymers.[49] The properties of the coordinating rare earth metal ions in these structures are not interfering, which allows the rational design of desired functional materials. Herein we report that upon employment of a ligand containing the aggregation induced emission (AIE) group as the blue (B) emitting component and the rare earth metal ions Eu^{3+} and Tb^{3+} as the red (R) and green (G) emission components, the RGB three color elements can be simply controlled *via* concentration. As a result, fluorescent white films

[a] College of Chemistry and Chemical Engineering, Xinjiang University, Urumqi, 830046, China. E-mail: hyhai97@126.com
[b] Beijing National Laboratory for Molecular Sciences (BNLMS), State Key Laboratory for Structural Chemistry of Unstable and Stable Species, College of Chemistry and Molecular Engineering, Peking University, Beijing 100871, China. E-mail: yunyan@pku.edu.cn, jbhuang@pku.edu.cn

† Electronic supplementary information (ESI) available. See DOI: 10.1039/c7tc01429e

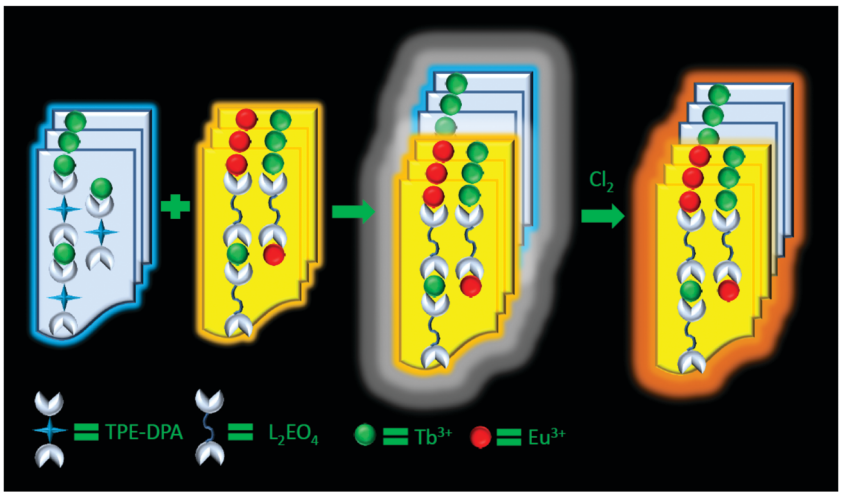

Scheme 1 Illustration of the fabrication of white emission films with rationally designed reversible coordination polymers.

with CIE coordinates of (0.335, 0.347) and external quantum efficiencies of up to 11.74% can be facilely fabricated. Specifically, the white emission solid film displays robust stability against temperature, environmental pH, and explosive chemicals, but exhibits specific sensitivity to Cl_2, manifesting the excellent potential of this white emission film for application as a luminescent material and a chemical sensor (Scheme 1). Furthermore, our work also shows that the judicious design of reversible coordination polymers may open up a new vista in materials science.

Experimental

Materials

Polyethyleneimine (PEI) (Aldrich, M_w = 10 000), $Eu(NO_3)_3{\cdot}6H_2O$, and $Tb(NO_3)_3{\cdot}6H_2O$ were used as received. TPE-DPA and L_2EO_4 were synthesized in our lab.[50] The substrates for the UV-vis spectroscopic investigations were made of quartz glass.

Methods

LBL film fabrication: the LBL films were prepared on substrates of quartz glass. The quartz glass substrates were cleaned in a mixture of $H_2SO_4 : H_2O_2$ (7 : 3) at 80 °C for 1 h, and washed with Milli-Q-water. The substrates were further cleaned using the RCA cleaning procedure in a $H_2O : H_2O_2 : NH_3$ (5 : 1 : 1) mixture. After washing with Milli-Q water and drying with air, the pre-cleaned quartz plates were immersed in a 10 mM polyethyleneimine (PEI) aqueous solution for 1 h to get a surface coated with a PEI monolayer. After Milli-Q water rinsing and air-drying, the greenish-blue LBL films were fabricated by alternating immersion of the modified substrates in PEI (10 mM) for 2 min and a solution of TPE (20 μM) for 15 min and $Tb(NO_3)_3{\cdot}6H_2O$ (10 mM) for 2 min. After each dipping, the plates were rinsed 3 times with Milli-Q water (1 min) and dried with air. The white emitting LBL films were fabricated by alternatingly immersing the blue-emitting film in PEI (10 mM) for 2 min and a mixed solution of $[Eu(NO_3)_3{\cdot}6H_2O/Tb(NO_3)_3{\cdot}6H_2O]$–$L_2EO_4$ for 5 min, followed by rinsing with Milli-Q water three times (1 min) and dried in air.

Characterization

Ultraviolet-visible (UV-vis) spectral measurements were carried out on a Shimadzu UV-1800 spectrophotometer in the range of 200–700 nm. Fluorescence spectra were recorded on a Hitachi F7000 Spectrometer in the range of 400–700 nm. AFM measurements were conducted on a Veeco Nanoscope IIIa AFM with a tapping mode under ambient conditions. Quantum efficiency measurements were carried out on an EI FLS980 lifetime and steady state spectrometer.

Results and discussion

Preparation of blue-green emission films

Blue-green emission films were first prepared by the LBL assembly of cationic polyethyleneimine (PEI), the anionic coordination supramolecular polymer made using the ditopic dipicolinic acid ligand containing tetraphenylethylene (TPE-DPA) and Tb^{3+} (Scheme 2a). TPE-DPA is soluble in water and emits weakly, but intense emission can be induced upon coordinating with Tb^{3+} owing to the aggregation induced emission nature of the TPE group.[51] However, the direct coordination of TPE-DPA and Tb^{3+} may lead to insoluble structures due to the formation of three dimensional networks at the coordinating stoichiometry of Tb^{3+}/TPE-DPA = 2/3.[52,53] To solve this problem, the multicharged TPE-DPA ligand was first assembled on the surface of the PEI layers, whereas the Tb^{3+} was assembled separately in the subsequent layer.

The successful growth of the multilayer films was conveniently monitored by UV-vis spectra. Fig. 1a reveals that the characteristic absorption of PEI at 212 nm[54] increases linearly with the number of trilayers, indicating the deposition of equal amounts of PEI/TPE/Tb^{3+} in each cycle. Fig. 1b shows that after 15 cycles of LBL assembly, stable blue-greenish emission was obtained on the quartz plate. Fluorescence spectra reveal the coexistence

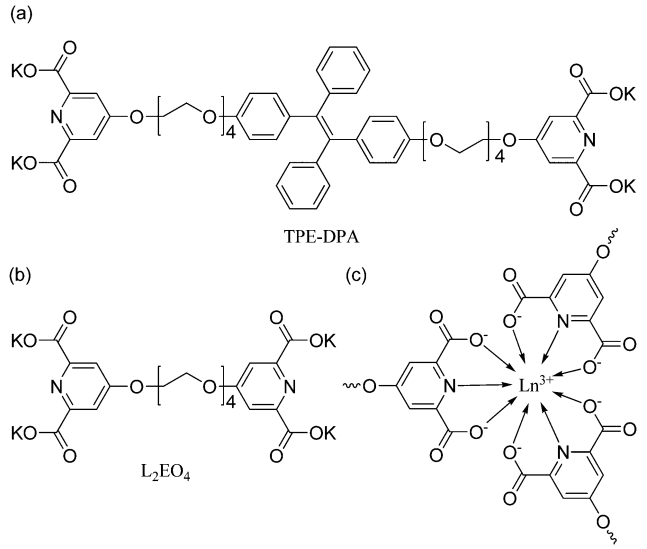

Scheme 2 (a) Structure of TPE-DPA; (b) structure of L_2EO_4; (c) demonstration of coordination between the head of L_2EO_4 and Ln^{3+}, where Ln represents rare earth metal ions Eu^{3+} and Tb^{3+}.

of a broad emission band of TPE-DPA peaked at 465 nm and the sharp emission for the coordinated Tb^{3+} at 545 nm in the LBL film (Fig. 1b).

Generation of white emission films

The CIE coordinates of greenish-blue (green and blue) emission of the $(PEI/TPE/Tb^{3+})_{15}$ film are (0.153, 0.234), which can be used to find the complementary color required for white emission. The line in Fig. 2b indicates that the required complementary color to the greenish-blue emission is orange. To this end, we tried to build an orange emission system with the mixed coordination polymer of Eu^{3+} and Tb^{3+}. In order to avoid any introduction of other emitters, the non-emitting dipicolinic bisligand 1,11-bis(2,6-dicarboxypyridin-4-yloxy)-3,6,9-trioxaundecane (L_2EO_4) (Scheme 2b) was employed to build the mixed coordinating system. Fig. 2a shows that the red emission of Eu^{3+}–L_2EO_4 and the green emission of Tb^{3+}–L_2EO_4 are not interfering in the mixed solution, and their respective emission intensities are proportional to their molar fraction. The CIE chromaticity coordinates for the mixed systems with various Eu^{3+}–L_2EO_4/Tb^{3+}–L_2EO_4 ratios are indicated in Fig. 2b. It is clearly seen that system F, which corresponds to the Eu^{3+}–L_2EO_4/Tb^{3+}–L_2EO_4 ratio of 175 μM/75 μM, locates on the white emission line. This indicates that the white light emitting films may be constructed by rationally controlling the layer thickness of PEI/TPE-DPA/Tb^{3+} and PEI/Ln^{3+}–L_2EO_4. (Ln^{3+}–L_2EO_4 (Scheme 2c) represents the mixture of Eu^{3+}–L_2EO_4/Tb^{3+}–L_2EO_4 with a molar ratio of 175 μM/75 μM.)[11,43,44]

Next, the (PEI/Ln^{3+}–L_2EO_4) layers were assembled on the basis of the blue emitting $(PEI/TPE/Tb^{3+})_{15}$ film. Fig. 3a shows a

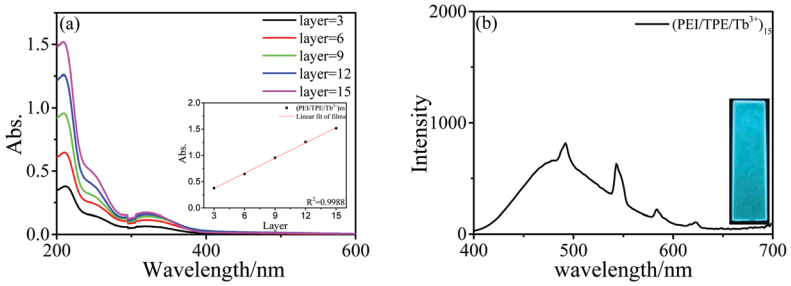

Fig. 1 (a) UV-vis absorption of the film of $(PEI/TPE/Tb^{3+})_{15}$; the inset shows a linear increase of the UV-vis absorption at 212 nm. (b) The emission spectra of $(PEI/TPE/Tb^{3+})_{15}$ in film upon excitations of λ_{ex} = 254 nm.

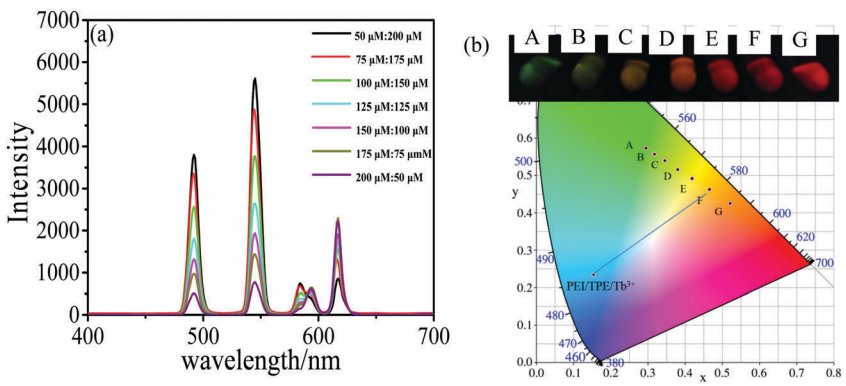

Fig. 2 Emission spectra of various mixed solutions of Eu^{3+}–L_2EO_4 and Tb^{3+}–L_2EO_4 (a) and the corresponding CIE coordinates (b). A–G correspond to the mixture with compositions of Eu^{3+}–L_2EO_4 : Tb^{3+}–L_2EO_4 = 50 μM : 200 μM, 75 μM : 175 μM, 100 μM : 150 μM, 125 μM : 125 μM, 150 μM : 100 μM, 175 μM : 75 μM, 200 μM : 50 μM, respectively. λ_{ex} = 254 nm for all the measurements.

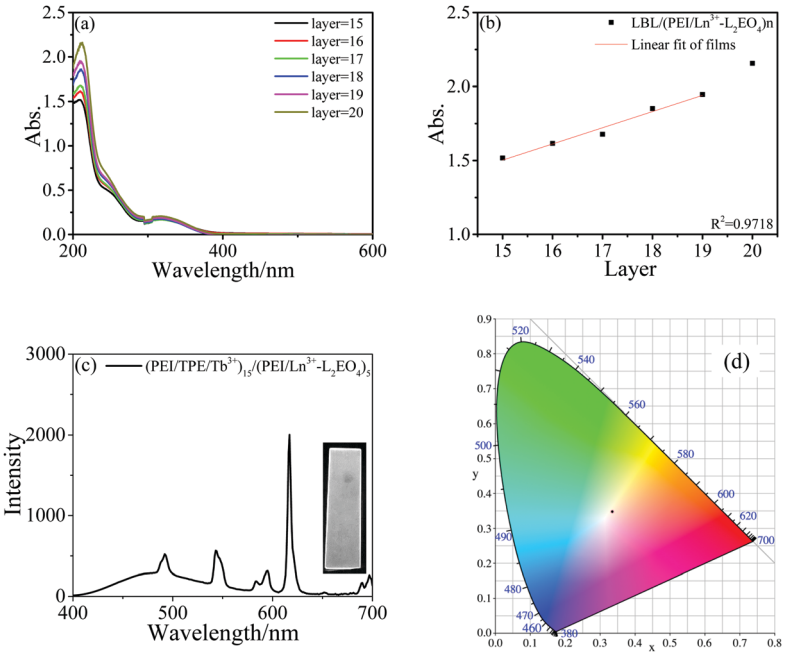

Fig. 3 (a) UV-vis absorption spectra of $(PEI/Ln^{3+}–L_2EO_4)_n$; (b) plots of the absorbance of 212 nm in (a) *vs.* the number of bilayers; (c) fluorescence spectrum of the $(PEI/TPE/Tb^{3+})_{15}/(PEI/Ln^{3+}–L_2EO_4)_5$ white emission film, the inset shows the photo of the film; (d) CIE coordinate of the white emission film.

linear increase of the characteristic absorbance of PEI upon continuous assembly of the $(PEI/Ln^{3+}–L_2EO_4)$ layers on the basis of the $(PEI/TPE/Tb^{3+})_{15}$ film, suggesting the homogeneous growth of the $(PEI/Ln^{3+}–L_2EO_4)$ film on the blue emitting film. White emission was obtained as the layer number of $(PEI/Ln^{3+}–L_2EO_4)$ amounts to 5. Fig. 3c shows the fluorescence spectrum of the white emitting film, where the characteristic emission corresponds to TPE-DPA (broad peak ranging from 400–590 nm), Tb^{3+}(sharp peaks at 475, 545 and 583 nm) and Eu^{3+} (sharp peaks at 595, 614, 689 and 697 nm) are clearly evidenced. The CIE coordinates for the emission of $(PEI/TPE/Tb^{3+})_{15}/(PEI/Ln^{3+}–L_2EO_4)_5$ was calculated to be (0.335, 0.347), which is close to the pure white emission with CIE coordinates of (0.333, 0.333).[55,56] Quantum efficiency measurement suggests that the white emission displays a high external quantum efficiency of 11.74%, which is sufficiently high when compared with film devices made with other tetraphenylethylene materials (5.3%)[57] and spirocyclic phosphine oxide (15%)[58] (Fig. S1, ESI†).

AFM measurements indicate that the thickness of the white emission film is about 49.5 nm (Fig. S2, ESI†). However, this nanometer-thick film displays excellent stability. As the temperature increases from 25 °C to 85 °C, the emission intensity only decreases slightly (Fig. 4a and b). With the temperature increasing, there are also no color changes in the digital photo. As the film was treated with solutions of pH ranging from 1 to 13 (Fig. 4c and d) or immersed into explosive solution, such as 2-amino-4-nitrophenol (ANP), 4-nitrophenol (NP), 4-nitrotoluene (NT), and 2,4,6-trinitrophenol (TNP) (Fig. 4e and f), no detectable color change was observed, too (Fig. 4c–f). These results indicate that the film can be a robust white emitting material that can resist severe environmental conditions.

Since white emission is very sensitive to any change in the RGB compositions, the film is expected to be useful in sensing of specific chemicals. Compared with the emissions from rare earth metals, that from the TPE group can be easily affected by chemicals since the ethylene bond of the TPE group may react with some specific reagents. This reaction will result in missing or weakening of the blue emitting element (B) from the RGB three primitive colors, thus leading to a color change from white to the complementary color of blue. Indeed, a distinct fluorescence change from white to orange was observed when the film was treated with Cl_2 gas (Fig. 4g), indicating that the blue emission from the TPE group was quenched. The change of the color is irreversible, suggesting that chemical reaction has occurred between Cl_2 and the TPE groups. Notice that the broad fluorescence peak featuring the emission of the TPE group disappears completely after treating with Cl_2, suggesting that Cl_2 have reacted with the ethylene bond of TPE, which can also be verified by UV-vis spectral measurement (Fig. S3, ESI†). In contrast, other gases, such as SO_2 (gas), CO_2 (gas), and H_2S (gas), can hardly trigger evident fluorescence changes (Fig. 4g and h). A weaker fluorescence change was noticed when the film was exposed to HCl gas, but the change is drastically different from that triggered by Cl_2, since the characteristic emission of the TPE group still remains (Fig. 4g). All these results clearly indicate that the white emission film constructed in this study is able to specifically detect Cl_2.

Conclusions

In summary, we have demonstrated the combination of aggregation induced emission and reversible coordination polymers

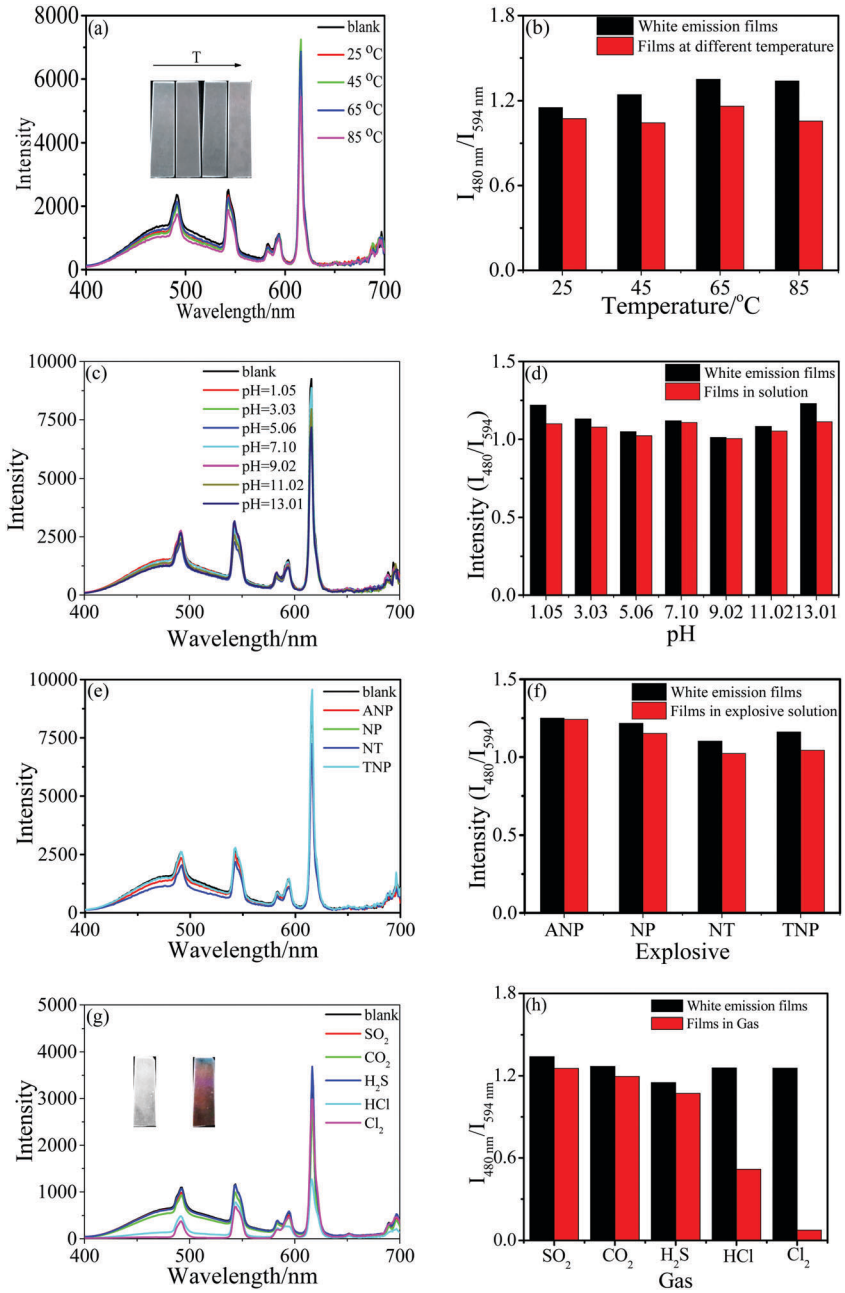

Fig. 4 The responsiveness of white emission films toward temperature and gas. (a) Emission spectral change of films with temperature; (b) the ratio of the emission intensity between 480 and 594 nm (I_{480}/I_{594}); (c) emission spectral change of films with pH; (d) emission intensity ratio between 480 and 594 nm (I_{480}/I_{594}); (e) emission spectral change of films for explosives (c = 5 mM); (f) fluorescence intensity ratio between 480 and 594 nm (I_{480}/I_{594}); (g) emission spectral change of films for gas; (h) fluorescence intensity ratio between 480 and 594 nm (I_{480}/I_{594}). Black bars represent the fluorescence intensity ratio of white emission films, while red bars represent measurements after films were exposed to various gases.

to construct white emitting solid thin films *via* LBL assembly. Owing to the dynamic nature of the reversible coordination polymers, controlled mixing of red emissive europium and terbium based coordination complexes becomes possible, which allows the generation of the complementary color of the blue-greenish emission of the aggregation induced emission. Upon the layer-by-layer assembly of the complementary color components onto a quartz plate, white emission thin films can be facilely achieved. The white emission exhibits CIE coordinates of (0.335, 0.347) and an external quantum efficiency of 11.7% at room temperature, which are very close to those of standard white emission (0.333, 0.333). In addition, the white film is very stable in a broad temperature and pH range, and is inert to explosive components, manifesting its great potential in the fabrication of white emitting devices. Furthermore, the white film displays specific detection of Cl_2, suggesting its possibility to be used as a chemical sensor. Compared with various white emission materials, the use of

reversible coordination polymers allows the rational design of white emission composition, which opens a new perspective for the development of functional white-light-emitting materials.

Acknowledgements

This work was supported by the National Natural Science Foundation of China (Grant No. 21573011, 21422302, 21362036) and National Basic Research Program of China (2013CB933800).

Notes and references

1 Z. M. Luo, G. Q. Qi, K. Y. Chen, M. Zou, L. H. Yuwen, X. W. Zhang, W. Huang and L. H. Wang, *Adv. Funct. Mater.*, 2016, **26**, 2739–2744.
2 H. Yoo, H. S. Jang, K. Lee and K. Woo, *Nanoscale*, 2015, **7**, 12860–12867.
3 X. Lian and B. Yan, *Dalton Trans.*, 2016, **45**, 2666–2673.
4 L. H. Zhi, Z. Y. Wang, J. Liu, W. S. Liu, H. L. Zhang, F. J. Chen and B. D. Wang, *Nanoscale*, 2015, **7**, 11712–11719.
5 S. Bhunia, N. Chatterjee, S. Das, K. Das Saha and A. Bhaumik, *ACS Appl. Mater. Interfaces*, 2014, **6**, 22569–22576.
6 B. S. Stromer and C. V. Kumar, *Adv. Funct. Mater.*, 2017, **27**, 1603874.
7 K. T. Kamtekar, A. P. Monkman and M. R. Bryce, *Adv. Mater.*, 2010, **22**, 572–582.
8 M. M. Shang, C. X. Li and J. Lin, *Chem. Soc. Rev.*, 2014, **43**, 1372–1386.
9 C. Tang, X. D. Liu, F. Liu, X. L. Wang, H. Xu and W. Huang, *Macromol. Chem. Phys.*, 2013, **214**, 314–342.
10 C. Y. Sun, X. L. Wang, X. Zhang, C. Qin, P. Li, Z. M. Su, D. X. Zhu, G. G. Shan, K. Z. Shao, H. Wu and J. Li, *Nat. Commun.*, 2013, **4**, 2717.
11 Q. Y. Yang, K. Wu, J. J. Jiang, C. W. Hsu, M. Pan, J. M. Lehn and C. Y. Su, *Chem. Commun.*, 2014, **50**, 7702–7704.
12 Y. Zhang, C. A. Xie, H. P. Su, J. Liu, S. Pickering, Y. Q. Wang, W. W. Yu, J. K. Wang, Y. D. Wang, J. I. Hahm, N. Dellas, S. E. Mohney and J. A. Xu, *Nano Lett.*, 2011, **11**, 329–332.
13 R. Z. Liang, D. P. Yan, R. Tian, X. J. Yu, W. Y. Shi, C. Y. Li, M. Wei, D. G. Evans and X. Duan, *Chem. Mater.*, 2014, **26**, 2595–2600.
14 A. R. Ramya, S. Varughese and M. L. P. Reddy, *Dalton Trans.*, 2014, **43**, 10940–10946.
15 Y. Ledemi, A. A. Trudel, V. A. G. Rivera, S. Chenu, E. Véron, L. A. Nunes, M. Allix and Y. Messaddeq, *J. Mater. Chem. C*, 2014, **2**, 5046–5056.
16 S. S. Babu, J. Aimi, H. Ozawa, N. Shirahata, A. Saeki, S. Seki, A. Ajayaghosh, H. Mohwald and T. Nakanishi, *Angew. Chem., Int. Ed.*, 2012, **51**, 3391–3395.
17 C. Vijayakumar, V. K. Praveen and A. Ajayaghosh, *Adv. Mater.*, 2009, **21**, 2059–2063.
18 V. Singh and A. K. Mishra, *J. Mater. Chem. C*, 2016, **4**, 3131–3137.
19 S. H. S. Koshari, J. L. Ross, K. Purnendu, I. E. Zarraga, R. Karthikan, N. J. Wagner and A. M. Lenhoff, *Mol. Pharmaceutics*, 2017, **14**, 546–553.
20 H. Hu, M. Pauly, O. Felix and G. Decher, *Nanoscale*, 2017, **9**, 1307–1314.
21 J. J. Richardson, M. Björnmalms and F. Caruso, *Science*, 2015, **348**, 411–423.
22 J. J. Richardson, J. W. Cui, M. Björnmalm, J. A. Braunge, H. Ejima and F. Caruso, *Chem. Rev.*, 2016, **116**, 14828–14867.
23 M. B. Oliveira, J. Hatami and J. F. Mano, *Chem. – Asian J.*, 2016, **11**, 1753–1764.
24 G. Schneider, G. Decher, N. Nerambourg, R. Praho, M. H. V. Werts and M. B. Desce, *Nano Lett.*, 2006, **6**, 530–536.
25 M. Lin, Y. Gao, T. J. Diefenbach, J. K. Shen, F. J. Hornicek, Y. I. Park, F. Xu and T. J. Lu, *ACS Appl. Mater. Interfaces*, 2017, **9**, 7941–7949.
26 T. Etrych, H. Lucas, O. Janoušková, P. Chytil, T. Mueller and K. Mäder, *J. Controlled Release*, 2016, **226**, 168–181.
27 Z. Y. Dong, L. Tang, C. C. Ahrens, Z. Y. Ding, V. Cao, J. T. Yan and W. Li, *Lab Chip*, 2016, **16**, 4601–4611.
28 P. Zhang, H. L. Li, J. J. Shi and J. Lu, *RSC Adv.*, 2016, **6**, 94739–94747.
29 T. Imaoka, H. Kobayashi, M. Katsurayama and K. Yamamoto, *Dalton Trans.*, 2015, **44**, 15116–15120.
30 T. H. Kim, D. Y. Chung, J. Y. Ku, I. Song, S. Sul, D. H. Kim, K. S. Cho, B. L. Choi and J. M. Kim, *Nat. Commun.*, 2013, **4**, 2637.
31 X. J. Zhang, C. H. Zhou, S. P. Zang, H. B. Shen, P. P. Dai, X. T. Zhang and L. S. Li, *ACS Appl. Mater. Interfaces*, 2015, **7**, 14770–14777.
32 Y. Yan, N. A. M. Besseling, A. D. Keizer, A. Marcelis, M. Drechsler, C. Stuart and A. Martien, *Angew. Chem., Int. Ed.*, 2007, **46**, 1807–1809.
33 L. M. Xu, Y. Y. Jing, L. Z. Feng, Z. Y. Xian, Y. Yan, Z. Liu and J. B. Huang, *Phys. Chem. Chem. Phys.*, 2013, **15**, 16641–16647.
34 L. M. Xu, L. Z. Feng, Y. C. Han, Y. Y. Jing, Z. Y. Xian, Z. Liu, J. B. Huang and Y. Yan, *Soft Matter*, 2014, **10**, 4686–4693.
35 L. M. Xu, L. X. Jiang, M. Drechsler, Y. Sun, Z. R. Liu, J. B. Huang, B. Z. Tang, Z. B. Li, M. A. Cohen Stuart and Y. Yan, *J. Am. Chem. Soc.*, 2014, **136**, 1942–1947.
36 H. Krass, G. Papastavrou and D. G. Kurth, *Chem. Mater.*, 2003, **15**, 196–203.
37 M. Schutte, C. Stolle and D. G. Kurth, *Supramol. Chem.*, 2003, **15**, 549–555.
38 D. G. Kurth, J. P. Lopez and W. F. Dong, *Chem. Commun.*, 2005, 2119–2121.
39 Y. Yan, A. A. Martens, N. A. M. Besseling, F. A. D. Wolf, A. D. Keizer, M. Drechsler, C. Stuart and A. Martien, *Angew. Chem., Int. Ed.*, 2008, **47**, 4192–4195.
40 Y. Yan and J. B. Huang, *Coord. Chem. Rev.*, 2010, **254**, 1072–1080.
41 Y. Yan, N. A. M. Besseling, A. D. Keizer and M. A. C. Stuart, *J. Phys. Chem. B*, 2007, **111**, 5811–5818.
42 Y. Yan, Y. R. Lan, A. D. Keizer, M. Drechsler, H. V. As, M. A. C. Stuart and N. A. M. Besseling, *Soft Matter*, 2010, **6**, 3244–3248.

43 L. Yang, Y. Ding, Y. Yang, Y. Yan, J. B. Huang, A. D. Keizer and M. A. C. Stuart, *Soft Matter*, 2011, **7**, 2720–2724.
44 Y. Ding, Y. Yang, L. Yang, Y. Yan, J. B. Huang and M. A. C. Stuart, *ACS Nano*, 2012, **6**, 1004–1010.
45 L. Zhao, Y. Yan and J. B. Huang, *Langmuir*, 2012, **28**, 5548–5554.
46 Z. Wu, J. B. Huang and Y. Yan, *Langmuir*, 2015, **31**, 7926–7933.
47 Y. Yan, Y. R. Lan, A. D. Keizer, M. Drechsler, H. V. As, M. A. C. Stuart and N. A. M. Besseling, *Soft Matter*, 2010, **6**, 3244–3248.
48 L. Yang, Y. Ding, Y. Yang, Y. Yan, J. B. Huang, A. D. Keizer and M. A. C. Stuart, *Soft Matter*, 2011, **7**, 2720–2724.
49 J. Y. Wang, A. H. Velders, E. Gianolio, S. Aime, F. J. Vergeldt, H. V. As, Y. Yan, M. Drechsler, A. D. Keizer, M. A. C. Stuart and J. V. D. Gucht, *Chem. Commun.*, 2013, **49**, 3736–3738.
50 T. Vermonden, J. V. D. Gucht, P. D. Waard, A. T. M. Marcelis, N. A. M. Besseling, E. J. R. Sudhölter, G. J. Fleer and M. A. C. Stuart, *Macromolecules*, 2003, **36**, 7035–7044.
51 J. Li, K. J. Shi, M. Drechsler, B. Z. Tang, J. B. Huang and Y. Yan, *Chem. Commun.*, 2016, **52**, 12466–12469.
52 L. M. Xu, M. Q. Xie, J. B. Huang and Y. Yan, *Langmuir*, 2016, **32**, 5830–5837.
53 L. Wang, W. Q. Wang and Z. G. Xie, *J. Mater. Chem. B*, 2016, **4**, 4263–4266.
54 X. M. Li, Y. H. Zhang, Y. L. Wu, Y. Duan, X. L. Luan, Q. Zhang and Q. An, *ACS Appl. Mater. Interfaces*, 2015, **7**, 19353–19361.
55 M. Partha, M. Debadrita and E. Prasad, *Chem. Commun.*, 2016, **52**, 4309–4312.
56 Z. Zhang, Y. H. He, L. Liu, X. Q. Lu, X. J. Zhu, W. K. Wong, M. Pan and C. Y. Su, *Chem. Commun.*, 2016, **52**, 3713–3716.
57 P. I. Shih, C. Y. Chuang, C. H. Chien, E. W. G. Diau and C. F. Shu, *Adv. Funct. Mater.*, 2007, **17**, 3141–3146.
58 J. Li, D. X. Ding, Y. T. Tao, Y. Wei, R. F. Chen, L. H. Xie, W. Huang and H. Xu, *Adv. Mater.*, 2016, **28**, 3122–3130.